A&A 458, 203–212 (2006)
DOI: 10.1051/0004-6361:20054778

Astronomy & Astrophysics

The "Príncipes de Asturias" nebula: a new quadrupolar planetary nebula from the IPHAS survey⋆

A. Mampaso[1], R. L. M. Corradi[2,1], K. Viironen[1], P. Leisy[2,1], R. Greimel[2], J. E. Drew[3], M. J. Barlow[4], D. J. Frew[5], J. Irwin[6], R. A. H. Morris[7], Q. A. Parker[5], S. Phillipps[7], E. R. Rodríguez-Flores[8,1], and A. A. Zijlstra[9]

(Affiliations can be found after the references)

Received 26 December 2005 / Accepted 10 July 2006

ABSTRACT

Context. The Isaac Newton Telescope Photometric Hα Survey (IPHAS) is currently mapping the Northern Galactic plane reaching to $r' = 20$ mag with typically 1″ resolution. Hundreds of Planetary Nebulae (PNe), both point-like and resolved, are expected to be discovered. We report on the discovery of the first new PN from this survey: it is an unusual object located at a large galactocentric distance and has a very low oxygen abundance.

Aims. Detecting and studying new PNe will lead to improved estimates of the population size, binary fraction and lifetimes, and yield new insights into the chemistry of the interstellar medium at large galactocentric distances.

Methods. Compact nebulae are searched for in the IPHAS photometric catalogue, selecting those candidates with a strong Hα excess in the $r' - H\alpha$ vs. $r' - i'$ colour–colour diagram. Searches for extended nebulae are by visual inspection of the mosaics of continuum-subtracted Hα images at a spatial sampling of 5×5 arcsec^2. Follow-up spectroscopy enables confirmation of the PNe, and their physico-chemical study.

Results. The first planetary nebula discovered via IPHAS imagery shows an intricate morphology: there is an inner ring surrounding the central star, bright inner lobes with an enhanced waist, and very faint lobular extensions reaching up to more than 100″. We classify it as a quadrupolar PN, a rather unusual class of planetary showing two pairs of misaligned lobes. From long-slit spectroscopy we derive T_e[NII] = 12 800 ± 1000 K, N_e = 390 ± 40 cm^{-3}, and chemical abundances typical of Peimbert's type I nebulae (He/H = 0.13, N/O = 1.8) with an oxygen abundance of 12 + log(O/H) = 8.17 ± 0.15. A kinematic distance of $7.0^{+4.5}_{-3.0}$ kpc is derived, implying an unusually large size of >4 pc for the nebula. The photometry of the central star indicates the presence of a relatively cool companion. This, and the evidence for a dense circumstellar disk and quadrupolar morphology, all of which are rare among PNe, support the hypothesis that this morphology is related to binary interaction.

Key words. planetary nebulae: general – ISM: abundances

1. Introduction

The INT/WFC Photometric Hα Survey of the Northern Galactic Plane (IPHAS) is an ambitious programme supported by an international collaboration among 15 institutes. The survey aims at producing a complete and detailed Hα map of the Galactic Plane, within the latitude range, $-5° \leq b^{II} \leq +5°$, north of the celestial equator. The survey will cover a total of 1800 square degrees of sky. It started in August 2003, with a target completion date of the end of 2006. It is estimated to take a total of 30 observing weeks (mostly during bright time), contributed by all three national communities involved – the UK, Spain and the Netherlands.

IPHAS makes use of the Wide Field Camera (WFC) of the 2.5 m Isaac Newton Telescope (INT) at the Observatorio del Roque de los Muchachos on La Palma, Spain. A narrow-band Hα filter (λ_c = 6568 Å; *FWHM* = 95 Å) and two broad-band Sloan r', i' filters are used for matched 120, 30, and 10 s exposures, respectively, spanning the magnitude range $13 \leq r' \leq 20$ for point sources. The survey area is covered in double pass, such that every pointing is repeated at an offset of 5 arcmin in both right ascension and declination. Pipeline data reduction and data distribution are handled by the Cambridge Astronomical Survey Unit (CASU `http://archive.ast.cam.ac.uk/`).

IPHAS is the first fully-photometric Hα survey of the Galactic plane, and it will complement the recently completed photographic survey of the southern Galactic plane performed with the AAO UK Schmidt Telescope (Parker et al. 2005) `http://www-wfau.roe.ac.uk/sss/halpha/index.html`.

IPHAS is expected to discover up to 50 000 new emission-line stars, including young stars (T Tau, Herbig AeBe stars, etc.), and evolved ones (post-AGB, LBVs, etc.), as well as different classes of interacting binaries (CVs, symbiotic stars, etc.) in addition to thousands of extended nebulae such as planetary nebulae, HII regions, SN remnants, H-H objects, etc. Further information on the objectives of IPHAS, its products, and early scientific results can be found in Drew at al. (2005) and in the public web site at `http://www.iphas.org/`.

1.1. IPHAS and planetary nebulae

One significant contribution of IPHAS will be in the field of planetary nebulae (PNe). The AAO-UKST Southern photographic Hα survey picked up nearly 1000 new PNe (Parker et al. 2006). IPHAS has a similar detection limit for extended objects but an improved spatial resolution, and it is estimated that IPHAS will discover several hundred new PNe, including very low surface-brightness objects and faint compact nebulae. The lower nebular surface brightnesses, relative to

⋆ The object, whose official name is IPHASX J012507.9+635652, is called as "Nebulosa de los Príncipes de Asturias" after its dedication by the Instituto de Astrofísica de Canarias to the Spanish Princes on the occasion of their wedding, which took place in Madrid on May, 22nd, 2004.

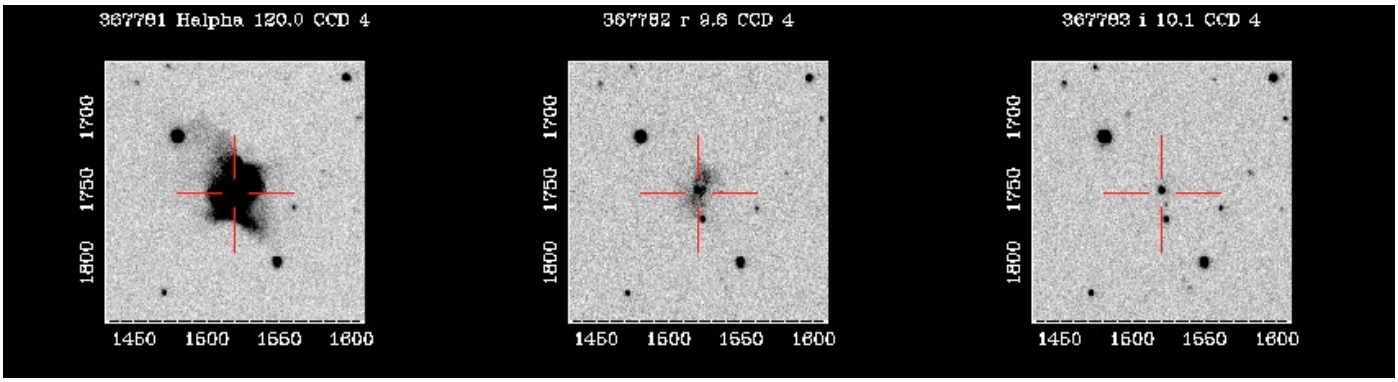

Fig. 1. Discovery images of the planetary nebula IPHAS PN-1 in Hα, r', and i' with exposures of 120, 10, and 10 s, respectively. Note that the Hα filter of IPHAS includes the [N II] lines at 6548 and 6583 Å which are more intense than Hα in this object (see text). Images are 1 arcmin on each side; North is up and East to the left.

already known PNe, will make studies of their central stars easier to carry out, ultimately enabling much better statistics to be obtained on the overall incidence of binarity (currently a major unknown; cf. Moe & De Marco 2006) and the frequency of different binary types. The two surveys together will also allow us to obtain better estimates of the PN population size in the solar vicinity and throughout the disc of the Galaxy, a figure which is intimately related to our understanding of the PN density per unit luminosity in spiral galaxies, the stellar death rate, PNe lifetimes, and their absolute luminosities (Buzzoni et al. 2006).

A number of the PNe discovered by IPHAS will be located along very interesting lines-of-sight, such as the direction of the Galactic anticentre, providing new targets to probe stellar properties and the chemistry of the interstellar medium at large galactocentric distances. For these reasons, a significant effort is being made, within the IPHAS collaboration, to perform a systematic search for ionized nebulae, including PNe. Two search techniques are used.

First, candidate compact nebulae are selected from the photometric catalogue that is automatically created by the IPHAS data reduction pipeline. Both stellar and quasi-stellar sources are detected, and we select those with a strong Hα excess in the IPHAS $r' - $ Hα vs. $r' - i'$ colour–colour diagram (see Drew et al. 2005; and Corradi et al. 2005). This allowed us to select 66 candidates in the data analyzed so far, corresponding to the observations obtained from 2003 to July 2004.

Second, extended nebulae which are not detected by the automated photometry are found by visual inspection of the IPHAS images. In particular, the CASU web interface includes analysis software which produces mosaics of continuum-subtracted Hα images at any spatial sampling. We adopt a spatial binning of 15×15 pixels of the WFC CCDs, corresponding to 5×5 arcsec^2, which allows us to get $S/N \sim 4$ at $F(\mathrm{H}\alpha) = 2 \times 10^{-17}$ erg arcsec^{-2} cm^{-2} s^{-1} in each rebinned spatial element. Preliminary analysis of a few square degrees led to the detection of 20 candidate PNe. An article with further details on the search methods will be published as soon as the scanning of a significant fraction of the IPHAS area is completed in a systematic way for both small and large nebulae. The main aim of the present article is to illustrate the kind of results that we aim to obtain from IPHAS in the field of ionized nebulae, and its follow-up observations, by presenting the case of the first planetary nebula discovered by the project. As well as being first to be found, this object is also a puzzle.

Spectroscopic and imaging observations for this object are presented in Sect. 2. Data analysis and results are in Sect. 3, which includes a physico-chemical analysis, a spatio-kinematical model for the inner nebula, and a discussion of the central star and the distance to the PN. A general discussion and main conclusions are presented in Sects. 4 and 5, respectively.

2. Observations

2.1. IPHAS

Figure 1 presents the Hα, r' and i' images of a nebulous object discovered during the analysis of the IPHAS photometric catalogue. The images were obtained on October, 13th, 2003 under seeing conditions of 1.0 arcsec *FWHM*. The object is located at RA(2000) = $1^{\mathrm{h}}\,25^{\mathrm{m}}\,7.9^{\mathrm{s}}$; Dec(2000) = $+63^\circ\,56'\,52''$. As no sources are catalogued in the SIMBAD database within 4 arcmin of these coordinates, this is a genuine new detection of a Galactic nebula. According to the nomenclature adopted by the collaboration (Drew et al. 2005), the source was given the name IPHASX J012507.9+635652, where X stands for "extended". We will abbreviate to IPHAS PN-1 hereafter. The nebula is a radio source detected by the NRAO VLA Sky Survey (Condon et al. 1998) with an integrated flux of 4.2 ± 0.5 mJy at 1.4 GHz. It was not resolved by the radio beam, implying a size smaller than $74'' \times 44''$. On the other hand, no CO nor mid- or far- (MSX and IRAS) infrared sources are associated with the nebula.

The Hα + [N II] image (Fig. 1 left panel, and Fig. 2) reveals a complex nebular morphology, consisting of:

- a relatively bright central star;
- an inner elliptical ring with semiaxes (at peak) of $3\farcs2 \times 1\farcs3$, with the long axis oriented at PA $\sim 160^\circ$;
- a pair of incomplete bright lobes. The "waist" of the lobes is at PA = 170° and has a size of $13''$, i.e. it is larger than the ring and tilted with respect to it. The lobes extend in a direction which is roughly perpendicular to the waist, show some deviations from axisymmetry, and decrease abruptly in brightness at a distance of some $20''$ from the centre;
- inside these lobes, apparently arising from the bright inner ring (but, again, not aligned with it), there is an elliposidal structure roughly centred on the central star (possibly another pair of inner lobes/bubbles), whose long axis is oriented at PA = 100° and has semiaxes of roughly $3\farcs3 \times 6\farcs5$.

Figure 2 shows the inner, brighter region of the nebula with the different structures labelled. The presence of nested bipolar structures is characteristic of a handful of PNe forming the morphological class of the so-called quadrupolar nebulae

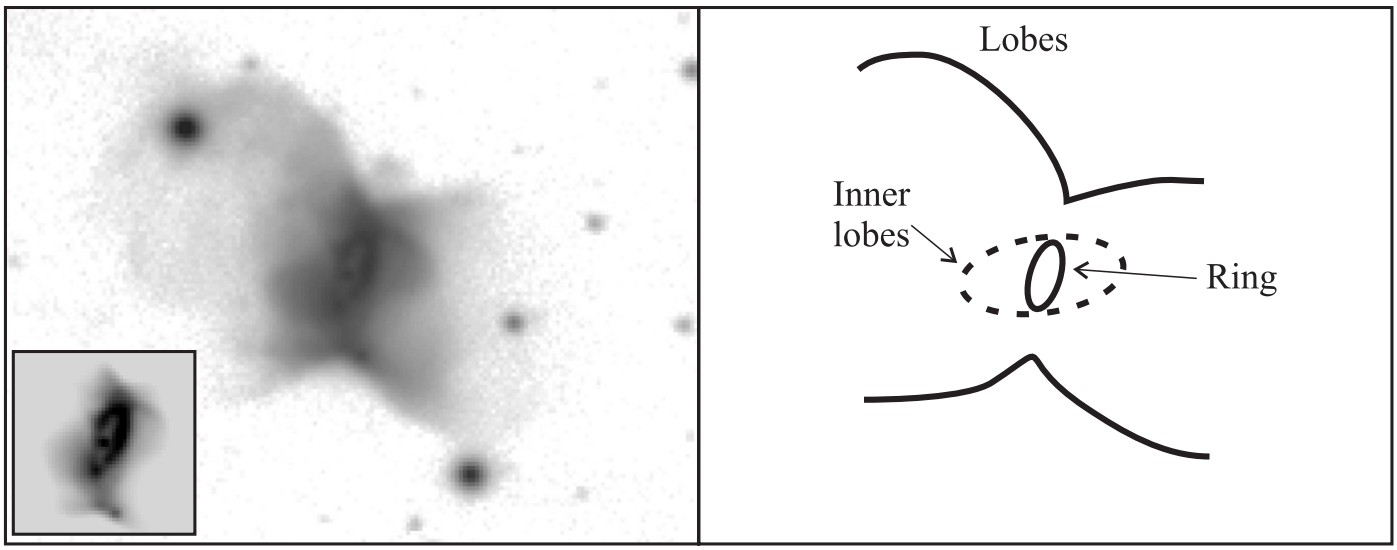

Fig. 2. (*Left*) Inner regions of IPHAS PN-1 in Hα + [N II] displayed with a logarithmic scale. The central star and elliptical ring are shown in the insert with a linear scale. (*Right*) Sketch showing the central elliptical ring, the main lobes and waist, and the tilted ellipsoidal inner lobes.

(Manchado et al. 1996). As this is a rare and puzzling class of PNe, we decided to take deeper images as well as spectroscopic data of the newly discovered nebula.

2.2. Other imaging

The object was imaged with the INT + WFC on August 4th, 2004 through the same Hα filter (total exposure time 18 min), an [S II] filter (λ_c = 6725 Å; *FWHM* = 80 Å; exp. time 30 min) and [O III] (λ_c = 5008 Å; *FWHM* = 100 Å; exp. time 18 min) filter. Seeing was 1.″4 in Hα and [O III] and 1.″0 in [S II]. The nebula is very faint both in [O III], where emission is limited to the zone of the ring and inner lobes, and in [S II], where basically only the ring is visible. As the Hα image does not reveal more details than the original one, this second set of images is not shown in this paper.

An additional Hα + [N II] image with a total exposure time of 1.5 h (9 × 600 s) was obtained with the INT + WFC on September 3rd, 2004. The night was photometric with seeing of 0.9 arcsec and the image was flux calibrated using the standard stars GD240 and Feige 110 (Oke 1990). This deep image, displayed in Fig. 3, reveals spectacular extensions of the outer lobes along their Eastern side, with only hints of a corresponding extension on the opposite side. The tip of the Eastern extension has the shape of an arrow and is located at a distance of 105 arcsec from the central star, at PA = 83°, i.e. in an axis perpendicular, within errors, to the waist. The projected symmetry axes of the different structures in IPHAS PN-1 rotate clockwise from the interior, the ring at PA = 160°, to the exterior, the inner lobes at PA = 100°, and the main lobes (including their faint extensions), at PA = 83°.

2.3. Follow-up spectroscopy

2.3.1. High resolution spectroscopy

IPHAS PN-1 was observed on October, 25th, 2004 with the 2.1 m telescope (Observatorio Astronómico Nacional, San Pedro Mártir, B.C. México) equipped with the MESCAL echelle spectrograph and a 90 Å wide Hα filter. The spectral reciprocal dispersion was 0.1 Å pix^{-1} over a spectral range from 6543 to 6593 Å. The slit width and length were 2.″0 and 5.′1, respectively. Exposures of 1200 and 1800 s were taken at PA = 0 and 57°, respectively, with median seeing of 1.6″ during the night.

Four lines were detected: [NII] $\lambda\lambda$ 6548, 6583 Å, He II 6560 Å and Hα. The bright Hα and [NII] 6583 Å lines could be measured along the inner ∼20″ of the nebula and are shown in Fig. 4. The rich spatio-kinematic structure seen in the 6583 Å line, that is presumably present in the Hα line, is smeared out by the higher thermal broadening associated with hydrogen. These data are analysed in Sect. 3.3, and further exploited in Sect. 3.4.

2.3.2. Low resolution spectroscopy

The nebula was observed on September, 23rd and 27th, 2004, with the 4.2 m WHT telescope (Observatorio del Roque de los Muchachos, La Palma, Spain) and the ISIS spectrograph. Two 1800 s exposures through the blue arm (Sep. 23rd) plus four 1800 s exposures through both the blue and red arms (Sep. 27th) were taken using gratings R300B (spectral dispersion of 0.86 Å pix^{-1} from 3500 to 6100 Å) and R158R (dispersion of 1.63 Å pix^{-1} from 6000 to 10 500 Å). The spatial scale of the instrument is 0.″2 pix^{-1} and the slit width and length were 0.″9 and 3.′7, respectively. The slit was positioned passing through the central star at PA = 180° (Sep. 23rd) and 125° (Sep. 27th), matching the parallactic angle at the middle of each observing period. Seeing was 0.″8 (Sep. 23th) and 1.″5 (Sep. 27th). Bias frames, twilight and tungsten flat-field exposures, arcs and exposures of the standard star G191-B2B (Oke 1990) were obtained. Spectra were reduced and flux calibrated using the standard IRAF packages for long-slit spectra.

3. Spectroscopic analysis

The [OIII] 4363 Å temperature sensitive line was measured with a S/N ratio of ∼30 in the WHT blue spectrum taken at PA = 180° on 23rd September 2004. It is clearly present in the spectrum at PA = 125° obtained 4 nights later, but because this was taken under worse seeing and bright (full moon) sky conditions, its profile is too noisy to justify a second measurement. In the

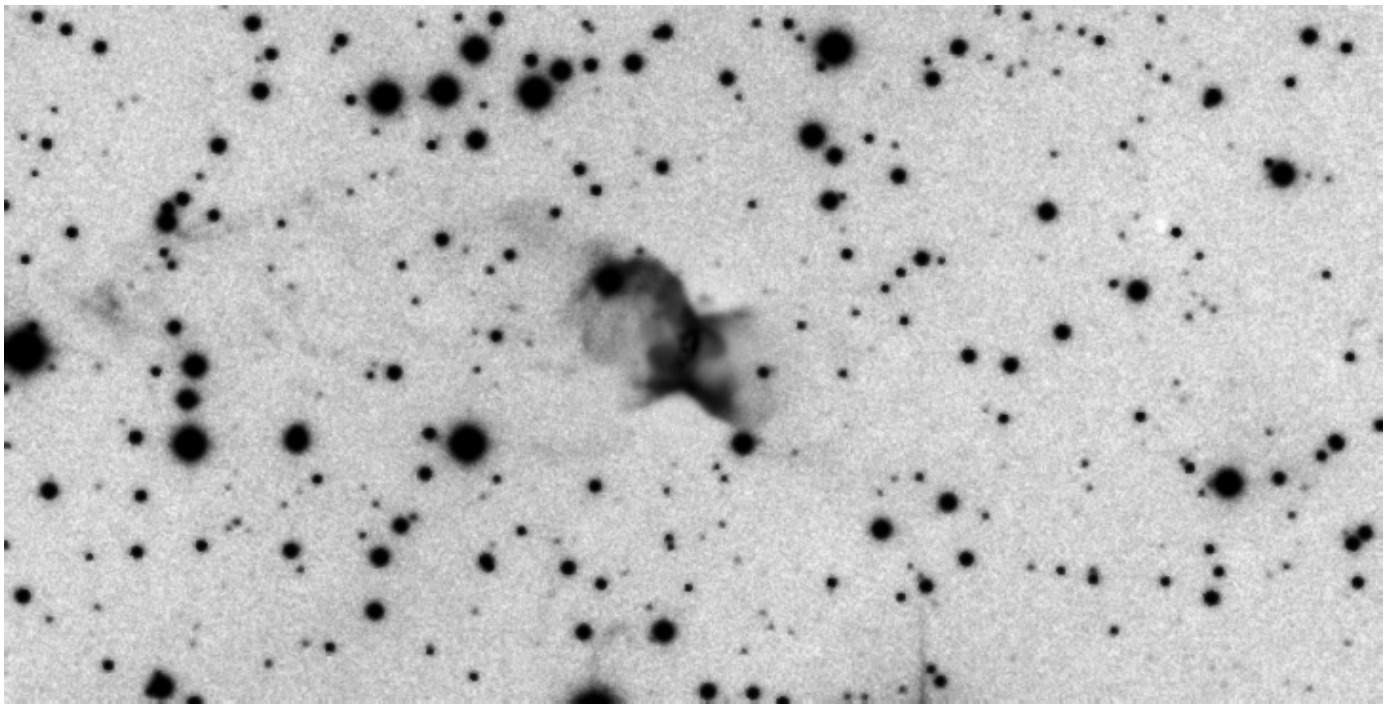

Fig. 3. IPHAS PN-1 in Hα + [N II] displayed with a logarithmic scale. The cuts are chosen as to highlight the extended low-level emission. The image size is $2' \times 4'$.

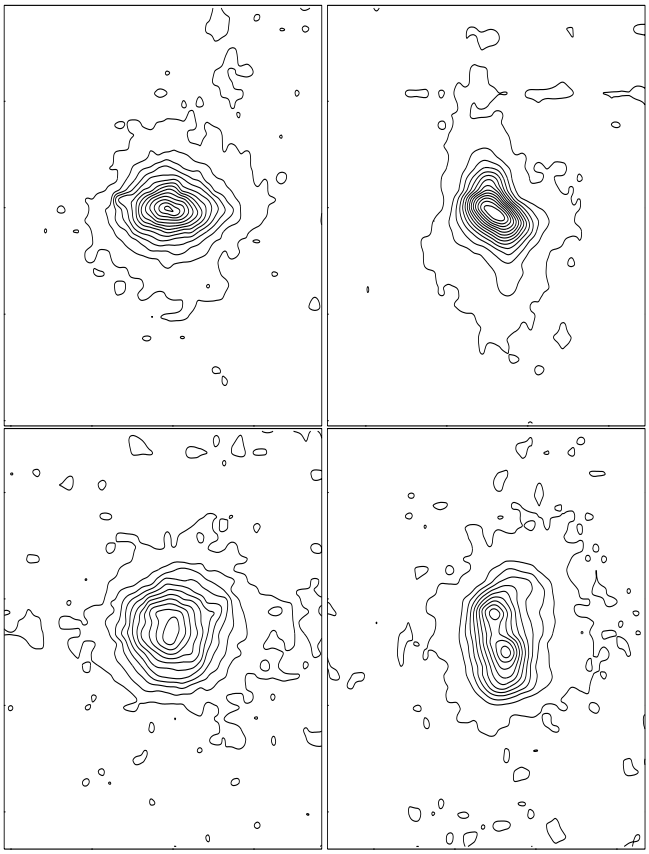

Fig. 4. Position-velocity maps for Hα (*left panels*) and [NII] 6583 Å (*right panels*) from the spectra at PA = 57° (*top panels*) and PA = 0° (*bottom panels*). Contours have been drawn from the 2-σ level to the maximum, linearly spaced and smoothed by block averaging by 2 × 2 pixels. The length of the vertical side of each box corresponds to 48″ (North is towards the bottom) whereas the horizontal side corresponds to 180 km s^{-1} (red is to the right).

following, we will assume for IPHAS PN-1 the T_e[OIII] determined from the spectrum of September 23rd, only, adopting a large uncertainty of 20% to account for both the formal errors (see below) and the fact that we implicitly assume an invariant T_e[OIII] across the nebula. Otherwise, the physico-chemical analysis described below is based on the lines measured in the complete (blue+red) spectra of September 27th, at PA = 125°.

Three nebular regions were selected: a central one extending ±0.8″ around the central star, plus two regions of 5.2″ located symmetrically with centres at 3.9″ NW and SE from the star. The latter correspond with the two bright sections of the inner ring, where line emission is stronger. No significant variations of extinction, density or temperature T_e[NII] were found between the NW and SE regions, and we averaged their spectra to further increase the S/N ratio. The resulting spectrum is shown in Fig. 5 and emission line fluxes are listed in Table 1. Quoted errors on observed fluxes include both the statistical poissonian noise and the systematic contributions of the wavelength and flux calibrations plus the continuum determination. Fluxes were extinction-corrected by using $c_{H\beta} = 2.0 \pm 0.1$ (the logarithmic ratio between observed and dereddened Hβ fluxes), determined from the observed Hα/Hβ ratio, and the reddening law of Cardelli et al. (1989) for $R_V = 3.1$. An average extinction can also be estimated comparing the radio and Hα fluxes (cf. Pottasch 1983). The raw integrated Hα + [N II] flux from the nebula, measured from the image in Fig. 3, is 1.20×10^{-12} erg cm^{-2} s^{-1} and the correction for [N II] $\lambda\lambda$6548, 6583 Å emission (using a flux ratio of [NII]/Hα = 3.2 as derived from the spectra; cf. Table 1) yields $F(H\alpha) = 3.75 \times 10^{-13}$ erg cm^{-2} s^{-1}. Comparing this with the measured radio flux (Sect. 2.1), and assuming that all the extinction is external to the object and that the Hα/[N II] ratio is constant along the nebula, we obtain $c_{H\beta} = 1.7 \pm 0.2$. This value is in fair agreement with the optical value, $c_{H\beta} = 2.0$, deduced above, and we will adopt the latter in the following.

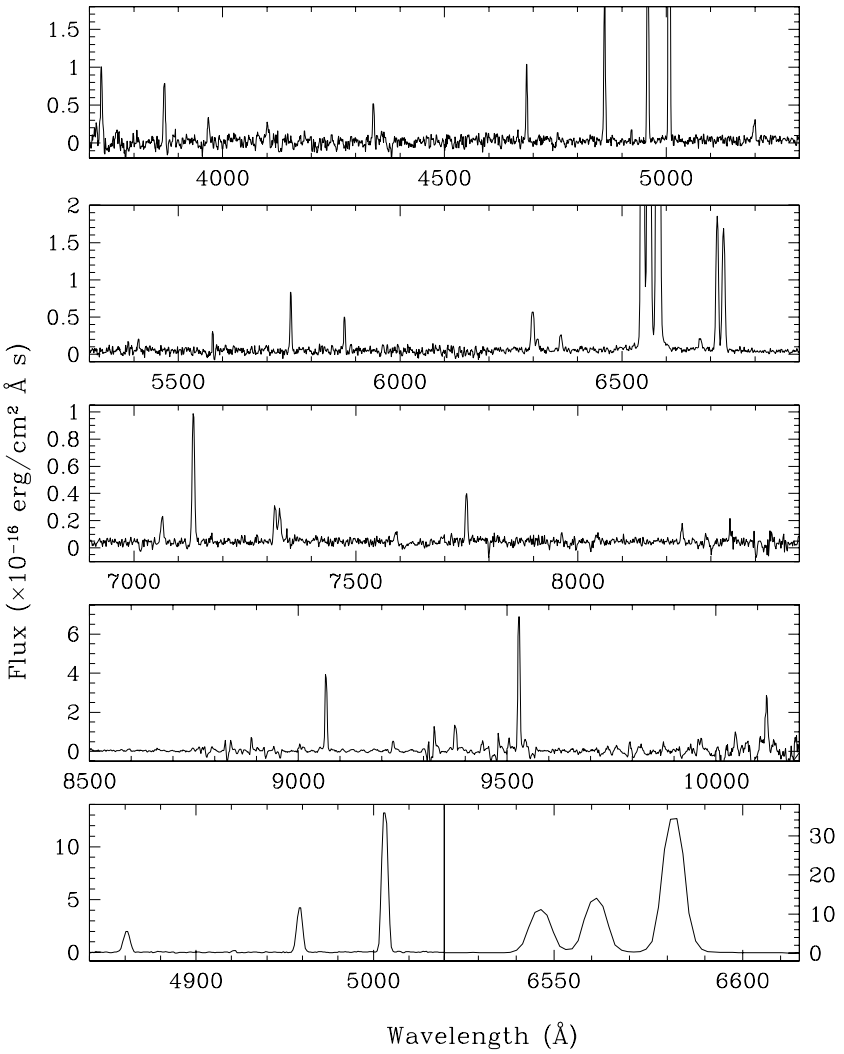

Fig. 5. WHT+ISIS spectrum of IPHAS PN-1 at PA = 125° (regions NW and SE co-added). The lowest panel shows full line profiles for the six strongest lines, Hβ, [OIII] $\lambda\lambda$ 4959, 5007 Å, Hα, and [NII] $\lambda\lambda$ 6548, 6583 Å.

3.1. Physical and chemical properties

The diagnostic ratios log(Hα/[N II]) = −0.50 and log(Hα/[S II])= 0.66 confirm the PN classification (Sabbadin et al. 1977). Its name, according to the standard IAU nomenclature, would be PN G 126.6+1.3, after its Galactic coordinates.

From the [O III], [N II], and [S II] line ratios, electron temperatures of T_e[OIII] = 14 100 ± 2800 K, T_e[NII] = 12 800 ± 1000 K and a density of N_e[SII] = 390 ± 40 cm^{-3} are obtained. Ionic and total abundances were calculated using a two-zone analysis and the NEBULAR IRAF package. Errors were consistently propagated through the calculations in the way described by e.g. Perinotto & Corradi (1998). Chemical abundances are shown in Table 2; associated errors include the uncertainties in the extinction, temperature, and the measured ionization correction factors (*icf*), in addition to the errors in the line fluxes. However, no uncertainties in the assumed extinction law nor in the *icf* scheme are considered. The latter was adopted from Kingsburgh & Barlow (1994; see also Perinotto et al. 2004, in particular for a discussion of the Sulphur abundance determination).

3.2. The central star

The central star's position and magnitudes, as measured from the IPHAS data, are RA(2000) = $01^h25^m07.93^s$; Dec(2000) = +63°56′52.7″; r' = 18.12 ± 0.02, and i' = 17.75 ± 0.02, respectively. The r' magnitude is likely to include nebular emission (cf. Fig. 1). The object is an infrared source (2MASS: Cutri et al. 2003) with J = 16.0 ± 0.1; H = 15.4 ± 0.1 and K_s = 14.45 ± 0.09. Assuming it suffers the same extinction as the nebular gas ($c_{H\beta}$ = 2.0, implying A_V = 4.1 mag) the dereddened colours $(J-H)_0$ = 0.17 and $(H-K_s)_0$ = 0.72 locate the object among the bulk of Galactic PNe nuclei and separate it convincingly from main-sequence stars, Mira variables and from the loci of thermal dust emitters (Ramos-Larios & Phillips 2005; see also Whitelock 1985). The object is also located in the PNe region of the near-infrared diagnostic diagram by Schmeja & Kimeswenger (2001). According to Whitelock (1985), the $(J-H)_0$ vs. $(H-K_s)_0$ colours are due to a combination of gas and dust thermal emission, line emission (e.g. HeI at 1.08 μm and H_2 at 2.12 μm) and photospheric emission from the central star. This makes it very difficult to derive physical information from the location of a particular object, unless one has detailed knowledge of its radio, infrared and optical properties. The optical spectrum of the star has been extracted from the WHT-ISIS data after subtracting the nearby nebular emission from two adjacent zones of 1.4 × 0.9 arcsec^2 located symmetrically at 2.6″ from the star, so that nebular lines are optimally supressed. The resulting stellar continuum is very red and almost featureless.

The central star shows a very strong Hα emission ($I_{H\alpha}$ = 2.5 × 10^{-15} erg cm^{-2} s^{-1}, integrated flux over an area of 1.4 × 0.9 arcsec^2) with a deconvolved Gaussian *FWHM* of 160 km s^{-1}.

Table 1. Observed and dereddened line fluxes for the WHT+ISIS spectrum at PA = 125° (normalized to Hβ = 100). Percentage rms errors are given within brackets.

Line Ident. (Å)	λ(Obs.)	Observed flux	Dereddened flux
[OII] 3726.0, 3728.8	3726.8	62.7 (6.1)	274.1 (9.0)
[NeIII] 3868.7	3868.6	46.0 (6.0)	174.8 (8.5)
[NeIII] 3967.5 + Hϵ	3968.0	18.2 (12.4)	61.7 (13.5)
Hγ 4340.5	4339.9	25.3 (6.8)	51.8 (7.5)
HeII 4685.7	4685.3	47.7 (4.0)	59.9 (4.1)
Hβ 4861.3	4860.9	100.0 (2.5)	100.0 (2.5)
[OIII] 4958.9	4958.4	194.8 (1.8)	173.2 (1.9)
[OIII] 5006.8	5006.4	630.3 (1.6)	530.3 (1.7)
[NI] 5197.9, 5200.2	5198.6	17.3 (8.5)	11.8 (8.7)
HeII 5411.6	5410.1	7.9 (18.4)	4.4 (18.6)
[NII] 5754.6	5753.6	37.5 (4.1)	16.1 (5.6)
HeI 5875.7	5874.7	24.7 (6.5)	9.8 (7.7)
[OI] 6300.3	6298.9	43.5 (5.1)	13.1 (7.4)
[SIII] 6312.1	6309.6	11.1 (21.2)	3.3 (21.9)
[OI] 6363.8	6362.3	14.1 (14.3)	4.1 (15.4)
[NII] 6548.0	6546.4	876.9 (1.5)	226.4 (6.3)
Hα 6562.8	6561.0	1116.0 (1.4)	285.6 (6.3)
[NII] 6583.4	6581.7	2732.1 (1.4)	690.6 (6.4)
HeI 6678.1	6676.7	13.8 (12.3)	3.3 (13.9)
[SII] 6716.5	6714.9	141.2 (2.1)	32.9 (6.9)
[SII] 6730.8	6729.2	127.4 (2.2)	29.5 (7.0)
HeI 7065.3	7063.5	17.3 (8.5)	3.3 (11.4)
[ArIII] 7135.8	7134.0	74.7 (2.8)	13.5 (8.2)
[OII] 7319.4	7317.7	19.8 (10.3)	3.2 (13.2)
[OII] 7330.3	7328.3	18.6 (9.7)	3.0 (12.8)
HeII 7592.7	7590.0	6.0 (26.2)	0.8 (27.7)
[ArIII] 7751.4	7749.2	24.8 (6.0)	3.1 (11.2)
HeII 8236.8	8234.8	8.2 (16.4)	0.8 (19.6)
[SIII] 9068.9	9066.4	288.3 (2.3)	19.0 (12.5)
P9 9229.0	9227.5	37.2 (10.9)	2.3 (16.6)
[SIII] 9531.0	9528.5	524.0 (2.9)	29.9 (13.3)
P7 10049.4	10047.2	70.7 (28.5)	3.5 (31.6)
HeII 10123.6	10121.6	221.1 (10.2)	10.8 (17.1)

The much fainter CaII lines at 8498, 8542 and 8662 Å (Fig. 6) show a *FWHM* velocity of ∼200 km s^{-1}. Their dereddened intensities are 7.1, 9.8 and 8.0 × 10^{-18} erg cm^{-2} s^{-1}, respectively (we have neglected the contribution of the three Paschen lines, Pa13, Pa15 and Pa16, blended with the CaII lines at our spectral resolution, given the faintness of the nearby Pa12, Pa14 and Pa17 lines; see Fig. 6). The observed width of the CaII lines is therefore similar to that of Hα, suggesting that both originate in the same region around the star. The intensity ratio for the CaII lines, 1.0:1.4:1.1, is very far from the expected ratio for optically thin emission, 1:9:5. This is common for objects where the triplet is in emission, and it indicates a high optical depth (Rodríguez et al. 2001). As in the case of the core of the PN He 2-428 discussed by the latter authors, the forbidden [CaII] lines at 7291 and 7324 Å are undetected at the core of IPHAS PN-1, indicating line quenching at very high densities ($N_e > 10^{10}$ cm^{-3}) as would occur in either a circumnuclear disc or a very dense circumstellar nebula.

3.3. Spatio-kinematical modelling

The [NII] λ 6583 Å data for PA= 0° described in Sect. 2.3.1 (Fig. 4) show two maxima separated by 4.5″ and 4.6 km s^{-1}. They correspond to the N and S sections of the inner ring, whose projected expansion velocity is therefore 2.3 km s^{-1}. If it is assumed this ring has a circular shape, its observed dimensions

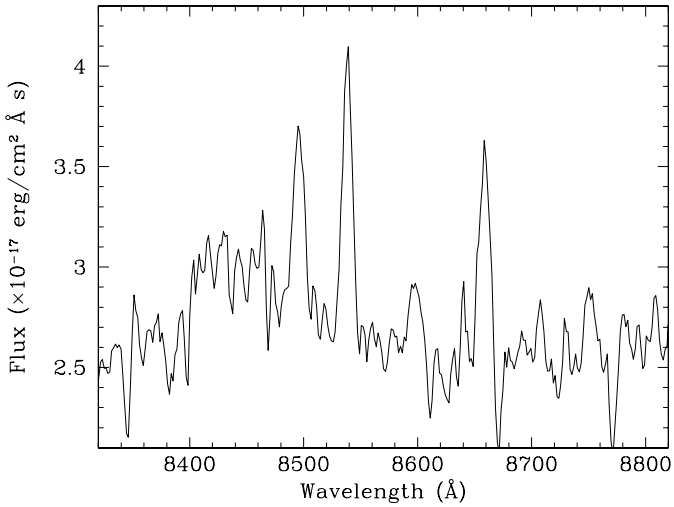

Fig. 6. CaII 8498, 8542 and 8662 Å emission lines at the central star. The nebular spectrum has been subtracted. The Pa14 and Pa12 HI lines at 8598 Å and 8750 Å, respectively, are barely detected.

(Sect. 2.1) would imply an inclination (the angle between the symmetry axis of the ring and the line of sight) of ∼68°.

A simple spatio-kinematical model was developed to fit the velocity data at PA = 57° (i.e. close to the symmetry axis of the inner nebula) and the shape of the central waist and bright lobes (Fig. 2). A geometrical description following Solf & Ulrich (1985) was used, where the space velocity of each gas particle is proportional to its distance from the central star; this produces a self-similar expansion in a so-called "Hubble-like" flow (Corradi 2004). The model also assumes axial symmetry and radial streamlines of gas. The resulting two-dimensional model is scaled to fit the size of the object, rotated into three dimensions about its symmetry axis and inclined to the plane of the sky to allow direct comparison with the image and spectrum. Synthetic geometrical shapes and velocity-position plots are generated and compared to the images and echelle spectrum. The model fit to the data is carried out visually after allowing the kinematical and geometrical parameters to vary over a large range of values; details of a similar modelling applied to the planetary nebula Mz 3 can be found in Santander-García et al. (2004). Results for the best fit model for IPHAS PN-1 are presented in Fig. 7.

An inclination angle of 55 ± 7° with respect to the line of sight was found for the axis of symmetry of the lobes, i.e. somewhat smaller than the inclination measured for the ring (68°). The waist expands at a velocity of 11 ± 3 km s^{-1}. The kinematic age of the nebula – less constrained by the modelling – is ∼2900 yr kpc^{-1}, with a large uncertainty spanning from 2000 to 4500 yr kpc^{-1}. Assuming the above mentioned Hubble-like expansion pattern, the lobe velocity at the poles would be as high as 220 km s^{-1}, a figure that can be tested by deeper observations able to reach the faint extremes of the lobes.

3.4. Distance

The object is located close to the Galactic plane at a favourable longitude (l = 126.°6) for obtaining an estimate of its distance via its systemic radial velocity, by assuming that it participates in the general circular rotation around the Galactic centre. The observed velocity of the nebula was measured from the higher-resolution echelle observations of the Hα and [N II] lines

Table 2. Ionic and total abundances of IPHAS PN-1. Percentage rms errors are given within brackets.

Ion/Element	Abundance	12 + log(X/H)	Type I[a]	Type I[b]
He^{+}/H	0.076 (8)			
He^{2+}/H	0.054 (7)			
He/H	**0.130 (11)**	**11.11 ± 0.05**	11.11[±0.016]	11.22[±0.015]
O^{0}/H	1.06E-05 (23)			
O^{+}/H	4.00E-05 (27)			
O^{2+}/H	6.48E-05 (49)			
icf(O)	1.42 (13)			
O/H	**1.49E-04 (34)**	**8.17 ± 0.15**	8.65[±0.15]	8.46[±0.17]
N^{+}/H	7.39E-05 (17)			
icf(N)	3.73 (44)			
N/H	**2.76E-04 (46)**	**8.44 ± 0.20**	8.72[±0.15]	8.50[±0.12]
Ne^{2+}/H	5.68E-05 (59)			
icf(Ne)	2.30 (60)			
Ne/H	**1.31E-04 (84)**	**8.12 ± 0.36**	8.09[±0.15]	
S^{+}/H	8.81E-07 (18)			
S^{2+}/H	2.57E-06 (65)			
icf(S)	1.18 (39)			
S/H	**4.07E-06 (62)**	**6.61 ± 0.27**	6.91[±0.30]	6.55[±0.25]
Ar^{2+}/H	5.83E-07 (35)			
icf(Ar)	1.87 (21)			
Ar/H	**1.09E-06 (41)**	**6.04 ± 0.18**	6.42[±0.30]	6.54[±0.04]

[a] Abundances for type I PNe from Kingsburgh & Barlow (1994). [b] Abundances for the three type I PNe with $D_{GC} \geq 11$ kpc from Costa et al. (2004). 1-σ dispersions of both samples are given within square brackets.

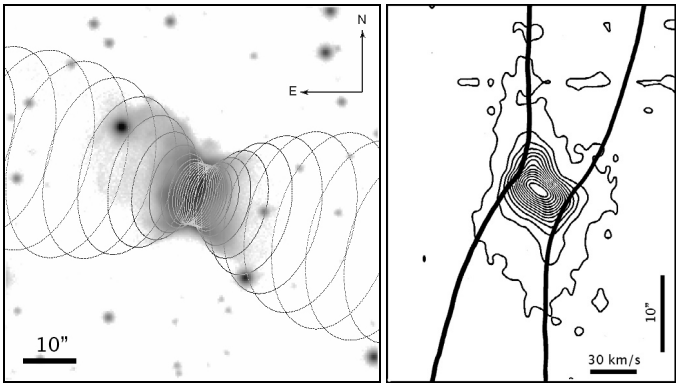

Fig. 7. (*Left*) Hα + [N II] image with superimposed ellipses representing circles inscribed on the walls of the geometrical shape used in the modelling. (*Right*) Observed [NII] position-velocity data for PA = 57° (isocontours) together with corresponding modelling results (thick lines).

in its central regions. This was found to be -83.5 ± 1.5 km s^{-1}, which translates to -71.1 ± 1.5 km s^{-1} when corrected to the Local Standard of Rest. On adopting a standard Galactic rotation curve (with a solar galactocentric distance of 8 kpc and a circular velocity of 220 km s^{-1}), the kinematical distance of the nebula is computed to be $7.0^{+4.5}_{-3.0}$ kpc. The relatively large error that we quote includes the error in the systemic velocity and, more important, an estimate of the velocity dispersion along the line of sight of all relatively young stars (age ≤3 Gyr, consistent with the hypothesis of a massive PN progenitor, see Sect. 4) located at a given galactocentric distance, assuming the same values as for the velocity dispersion ellipsoid in the solar neighbourhood (Nordström et al. 2004). This distance is only an estimate, as it comes from a simplified treatment of the dynamics of our Galaxy, but clearly points to a very large galactocentric distance of the nebula, namely $D_{GC} = 13.4^{+4.1}_{-2.5}$ kpc.

The distance can also be obtained from an extinction-distance relationship (e.g. Kaler & Lutz 1985) for the field. The SIMBAD astronomical database was used to extract all available photometric and spectroscopic information for stars within 60′ of the PN. Spectroscopic parallaxes were determined after adopting the intrinsic colours and absolute magnitudes for each spectral class from Schmidt-Kaler (1982). Figure 8 shows the trend, based on a linear least-squares fit to the early-type (OBA) stars in the field with best-quality data. The upper dashed line shows the asymptotic reddening in this direction (Schlegel et al. 1998) and the lower line is the reddening determined from the Balmer decrement for the PN.

A monotonic relation of reddening versus distance is seen for this field, although with considerable scatter. Using the observed reddening to the PN ($A_V = 4.1 \pm 0.10$), we obtain a distance of $D = 5.9 \pm 2.2$ kpc. The error on the distance is estimated following the approach of Kaler & Lutz (1985), and is probably optimistic as it does not account for any internal reddening in the nebula (if present, D is overestimated). The diamond in Fig. 8 is the intermediate-age open cluster NGC 559 (Ann & Lee 2002), while the point at $D = 8$ kpc is the high-mass X-ray binary V635 Cas (Negueruela & Okazaki 2001). The point at lower right (open circle) is the B8 Ib star NGC 559#14 (Lindoff 1969), that is not actually a member star of NGC 559. The adopted spectral type is from Sowell (1987) which places it far off the observed trend, and so it is excluded from the fit. However if the star is a bright giant (luminosity class II) rather than a Ib supergiant, the star would fall on the trend for the field.

Another distance estimation uses the empirical Hα surface brightness – radius relation which has been recently calibrated with PNe having accurate distances determined using a primary method (Frew et al. 2006; an early version of this relation is presented by Pierce et al. 2004). The technique requires an accurate determination of the dimensions of the main body of a PN, excluding any outer halos. For round and elliptical PNe, the adopted dimensions (used to calculate the mean surface brightness) are easily estimated. However, for bipolar nebulae, estimating the size is more problematic, so the surface brightnesses have a greater than average error. The main body of

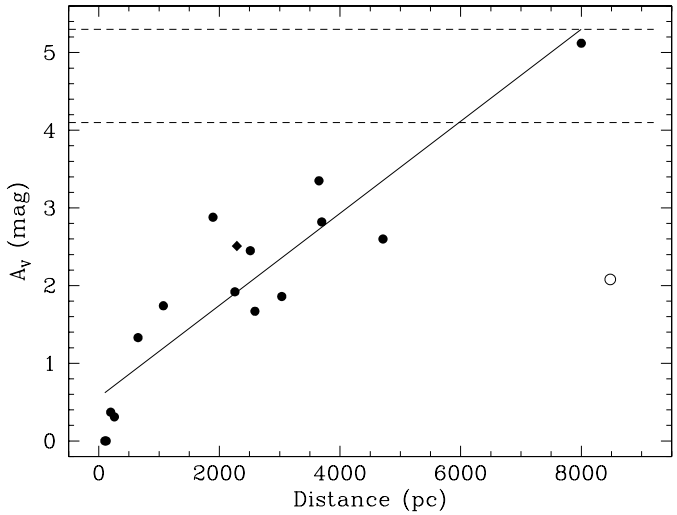

Fig. 8. Extinction-distance diagram for the field around IPHAS PN-1. The trend line is based on a least squares fit to the field stars with best quality data. The upper dashed line shows the asymptotic reddening in this direction and the lower dashed line is the reddening determined from the Balmer decrement for the PN (see text).

IPHAS PN-1 was roughly fitted by an ellipse to get dimensions of $21'' \times 12''$, and, using the total integrated Hα flux from Sect. 3, and the relation of Frew et al. (2006) for a subset of well-studied bipolar PNe, a distance, $D = 5.8 \pm 1.7$ kpc is estimated. This is in excellent agreement with both the extinction distance and the kinematic determination. In the following we will adopt the kinematical values, namely $D = 7.0$ kpc and $D_{\rm GC} = 13.4$ kpc.

The object is therefore located just outside the most distant spiral arm in that direction, the Perseus+1 arm (Vallée 2002) where current star formation activity is evidenced by the presence of young open clusters, OB associations, and HII regions (Kimeswenger & Weinberger 1989). Assuming for the whole nebula the inclination of 55° measured for the inner regions (Sect. 3.3), a size of 4.3 pc is derived for the Eastern lobe, making IPHAS PN-1 one of the largest PNe known. Its age is also very large: using the expansion velocity determined in Sect. 3.3, we obtain ∼20 000 yr for the nebula. The mass of the nebula can be estimated using the total Hα flux calculated above, and results in a nebular mass of $\sim 0.05\ M_\odot$, i.e. towards the lower end of typical PNe masses (cf. Pottasch 1983) and similar to He 2-104 and other bipolar nebulae believed to be produced by binary (or symbiotic) stars (Corradi & Schwarz 1993).

3.5. Binarity

It appears that the exciting star of IPHAS PN-1 belongs to a binary system: at the assumed distance and reddening, its observed i', J and H magnitudes (where nebular contamination is expected to be minor; Sect. 3.2) imply absolute magnitudes $M_{i'} = +0.9$, $M_J = +0.6$, and $M_H = +0.4$. The absolute V magnitudes for the hot central stars of evolved bipolar PNe (of which this is an example) range from $M_V = +5.0$ to $+7.5$ (Phillips 2005) equivalent to $M_{i'} \approx +5.3$ to $+7.8$, i.e. more than 4 mag fainter than observed. The discrepancy remains even if the distance is reduced to our lower limit of 4 kpc. Since the star appears almost perfectly at the centroid of the nebula, it is very unlikely that there is a line-of-sight projection.

We can use the implied $(J-H)_0$ and $(i'-J)_0$ colours of the nucleus to take this discussion further. We have derived $(J-H)_0 \simeq 0.2$, $(i'-J)_0 \simeq 0.3$: these roughly match expectation for a mid-F star, irrespective of luminosity class (cf. the synthetic photometry tabulated by Pickles (1998), giving $J-H = 0.2$–0.3 and $I_C - J \simeq 0.3$ at F5, for luminosity classes V-III). But it is clear that at a distance of 7 kpc, the mid-F companion would have to be of luminosity class III ($M_V = 1.6$ is given by Schmidt-Kaler 1982 for F5 III, cf. ∼1.5 implied for the central star in this case). At the lower limiting distance of 4 kpc the luminosity falls to a value not so far above that of a dwarf star ($M_V = 3.5$ from Schmidt-Kaler 1982, versus ∼2.7 here, at the nearer distance). A mid-F companion is thus the simplest option, and would not require much of a contribution to the red/NIR flux from accretion. In this circumstance, the source of the observed CaII IR triplet emission can be either irradiation of the companion, or a circumnuclear disc in which accretion at rates typical of high-state cataclysmic variables ($M_V \sim 4$, and neutral colour, Warner 1995) would not be detected. On the other hand, if e.g. NIR spectroscopy were to fail to confirm an F-star photosphere, then the more exotic scenario of light from both an evolved later-type companion and a relatively luminous accretion component would have to be considered (for all distances in excess of the 4 kpc minimum): such a system could resemble the old nova, and extreme dwarf nova, GK Per ($M_V \sim 1.6$ in outburst). In either case, there is no escaping the need to model this PN nucleus as a binary, and there is a significant likelihood that the binary is a relatively close one, with a period on the order of a day, so as to permit either significant irradation of the companion or a semi-detached configuration leading to mass transfer and accretion.

If the nuclear binary period is not short, dense circumstellar gas within a passive disk or similar remains a necessity as discussed in Sect. 3.2. High resolution imaging (e.g. with *HST*) might reveal this.

4. Discussion

The group of quadrupolar PNe is composed of only eight objects: five nebulae originally identified by Manchado et al. (1996; K 3-24, M 1-75, M 2-46, M 3-28, and M 4-14), one (NGC 6881) by Guerrero & Manchado (1998), a further one (NGC 4361) by Muthu & Anandarao (2001), plus NGC 2440 (Cuesta & Phillips 2000). All of them show an enhanced waist and two pairs of differently-aligned bipolar lobes, except in NGC 4361 whose nature as a quadrupolar PN is doubtful. IPHAS PN-1 is morphologically very similar to M 2-46 and M 1-75 but also to the bipolar PNe A 79 and He 2-248 – the latter are rather evolved nebulae, excited by binary stars (Rodríguez et al. 2001).

The origin of quadrupolar nebulae is important for the theories of PNe formation and evolution because they pose a strong challenge to the paradigm of the Generalized Interacting Stellar Winds (GISW, Balick & Frank 2002). GISW is not able to account for the formation of quadrupolar (nor multipolar and point-symmetric) nebulae and further physical processes such as external torques of a close binary companion or strong magnetic fields in the wind ejecta are required. Furthermore, there is an unsolved evolutionary problem in that bipolar, quadrupolar and multipolar morphologies are in the majority among proto-PNe and young PNe (Sahai & Trauger 1998), whereas round and elliptical geometries are, on the contrary, much more frequent both among PNe in general (Manchado 2004) and among their precursor AGB shells (cf. Sahai 2004). The process that transforms a spherical AGB envelope into an aspherical (but axisymmetric) object, like a quadrupolar PN, represents

a major challenge for the theories of post-main-sequence evolution (Sahai & Trauger 1998).

Models proposed for quadrupolar PNe are varied: a precessing binary system ejecting two bipolar shells (Manchado et al. 1996); an helicoidal precessing jet (Guerrero & Manchado 1998); magnetized, misaligned winds from a star and disc system (Blackman et al. 2001); and the precession of warped discs (Livio & Pringle 1997; Icke 2003). The one item in common with all models is the required presence of a binary system, although no evidence exists for that in the known sample of quadrupolars. Here, the evidence for binarity is compelling. Whether the binary is actually experiencing mass transfer is not so clear at this point. Nevertheless, as discussed in Sects. 3.2 and 3.5 above, there remains the possibility also of a very dense circumnuclear shell or disc in IPHAS PN-1, in spite of the fact that the nebula is rather old: it is hard, otherwise, to understand the widths and relative strengths of the CaII IR triplet components.

The chemistry of IPHAS PN-1, presented in Sect. 3.1, shows that it is a type I PN, with He/H = 0.13 ± 0.01 and N/O = 1.8 ± 0.6. The O abundance is remarkably low (Table 2, but notice the large associated error caused by the uncertain T_e[OIII]) and similar to the PNe with high-mass progenitors discussed by Marigo et al. (2003). However, we note that the Kingsburgh & Barlow (1994, KB94 in the following) *icf* scheme may break down for extreme type I nebulae such as IPHAS PN-1 and NGC 6302. Heavy elements in the latter nebula are spread across a much wider range of ion stages than for "normal" PNe. Using just the O^+ and O^{2+} abundances for NGC 6302 from Table 9 of Tsamis et al. (2003), equation A7 of KB94 predicts an *icf*(O) of 1.62. However, the O IV] λ1401-based abundance of O^{3+} was alone found by Tsamis et al. to be 82% of the $O^+ + O^{2+}$ abundance, with the *icf*(O) for stages higher than O^{3+} estimated by them to be 1.37, using equation A9 of KB94. As a result, Tsamis et al. obtained an overall oxygen abundance for NGC 6302 that was a factor of 1.6 larger than would have been estimated based just on the O^+ and O^{2+} abundances. Even this may be an underestimate, since NGC 6302 exhibits strong near-IR coronal line emission from highly ionized species (e.g. [Si VII] 2.48 μm and [Si IX] 3.93 μm; see Casassus et al. 2000), suggesting that highly ionized stages of oxygen may also be present. Since IPHAS PN-1 has a similar morphology and He II/Hβ ratio to NGC 6302 (Matsuura et al. 2005), the O/H abundance ratio listed in Table 2 could be a lower limit. Infrared spectroscopy of the [O IV] 25.89-μm line, as well as spectra covering the near-IR coronal lines, could be useful in helping to constrain the oxygen abundance.

From Figs. 11 and 12 of Marigo et al. (2003); Ma03 in the following), a progenitor mass of 2.5 $\rightarrow$ 3 $M_\odot$ would be estimated for IPHAS PN-1. But it is important to note that the object occupies an anomalous zone in the He/H vs. N/O diagram, where models with initial solar metallicity and masses up to 5 $M_\odot$ fall short by a factor >3 in reproducing the observed N/O, while the models with initial LMC metallicity overestimate He/H by >25%, a figure well outside the He/H error bar. Interestingly, IPHAS PN-1 is not alone in this "forbidden" zone of the He/H vs. N/O diagram: two other quadrupolar PNe are there, NGC 2440 (Ma03) and M1-75 (Perinotto et al. 2004). In addition, two type I PNe from the Ma03 article, NGC 5315 and NGC 6537 also lie in the same area of this diagram. In fact, the group of type I PNe studied by KB94 has average values of He/H = 0.13 and N/O = 1.2, i.e. they are also located in roughly the same area of the Ma03 diagram, pointing to a lack of plausible models for this kind of object (notice, however, that the Ma03 models do reproduce the abundances of the most extreme type I bipolars in their sample, i.e. those with He/H $\geq$ 0.15). With these considerations, we estimate that the progenitor of IPHAS PN-1 was an intermediate mass star (2.5 $\rightarrow$ 3 $M_\odot$) with solar metallicity or lower.

Let us compare now IPHAS PN-1 with the other known quadrupolar PNe. The first thing to note is that the quadrupolars are not a chemically homogeneous group: for the six PNe where adequate data exist, two are of type I (M 1-75 and NGC 2440), two of type II (M 4-14 and NGC 6881), one doubtful object (M 2-46) and one type IV (Halo) PN, NGC 4361 (but see above about its unclear classification). (References for the chemical abundances for these objects can be found in Torres-Peimbert et al. 1990; Perinotto 1991; Koeppen et al. 1991; Ma03; and Perinotto et al. 2004.) IPHAS PN-1 is the most extreme type I nebula (in He abundance and N/O ratio) of the known quadrupolars.

Table 2 compares IPHAS PN-1 with two type I samples: a) the group of 11 objects measured by KB94, all but one located at $D_{GC}\leq$11 kpc, and b) three PNe from Costa et al. (2004) having the largest D_{GC} in their sample: M 1-18, located at 10.9 kpc, M 3-3, at 12.4 kpc, and M 3-2, at 14.1 kpc (note that these authors adopt a solar galactocentric distance of 7.5 kpc). Subject to the caveat that unaccounted-for high ion stages could be present (see above), the abundances for IPHAS PN-1 in Table 2 are generally lower than for PNe in both the a) and b) samples, indicating a lower metallicity progenitor, and therefore in qualitative agreement with the large D_{GC} of 13.4 kpc estimated above. Costa et al. (2004) present a detailed study of chemical abundances for PNe towards the galactic anticentre. Their main conclusion, a flattening of the O/H gradient at large ($\gtrsim$11 kpc) galactocentric distances, is however hampered by the large observational dispersion (0.3 dex) for those distant objects. Clearly, more objects and better determined abundances and distances are needed to confirm this flattening. IPHAS PN-1 is an important PN in this respect: its O/H is the second lowest (after K 3-68; cf. Fig. 4 in Costa et al. 2004) and its D_{GC} one of the largest for which reliable data exist[1]. In fact, the low O/H measured for IPHAS PN-1, even allowing for an *icf*(O) enhanced from 1.5 (Table 2) to 2.4 (were it identical to NGC 6302; see above), is consistent with the galactic gradients found from PNe (-0.05 dex kpc^{-1}; Costa et al. 2004) and early B stars (-0.07 dex kpc^{-1}; Rolleston et al. 2000) at the galactocentric distance determined for the object. This lends support to models where the oxygen abundance gradient has a constant slope (Henry & Howard 1995).

5. Conclusions

The INT Photometric Hα Survey (IPHAS) is currently mapping the Northern Galactic Plane at unprecedented depth and spatial resolution. Hundreds of new planetary nebulae are awaiting discovery in the IPHAS photometric catalogue and its combined mosaic images. Here we have presented a morphological and physico-chemical study of the first PN discovered, IPHASX J012507.9+635652. This is an unusual nebula composed of a compact elliptical ring, inner lobes and waist, and faint outer bipolar lobes extending up to more than 100″ from the central star. The source likely belongs to the group of quadrupolar nebulae, with only eight other members known so far, and further

[1] An additional very distant PN has been recently found from the IPHAS survey: it is a type II object with O/H = 8.5 and it is very likely located beyond 14 kpc from the Galactic centre (Mampaso et al. 2005).

high spatial-resolution observations, and high-resolution spectroscopy of the nebula are desirable in order to unambiguously determine its quadrupolar nature. Broad Hα and CaII emission lines are detected from the central star, indicating the presence of very high densities ($N_e > 10^{10}$ cm^{-3}) from a thick circumstellar shell or disc. This, together with the photometric properties of the central star, make unavoidable the presence of a binary nucleus, the first evidence for this among the quadrupolars. Whether there is an active or a passive disk (or some other geometric structure) cannot be decided with the data at hand. The inner nebula is heavily reddened ($A_V = 4.1$ mag), with low densities (N_e[SII] = 390 ± 40 cm^{-3}) and rather high temperatures (T_e[OIII] = 14 100 ± 2800 K, T_e[NII] = 12 800 ± 1000 K). The chemistry is typical of extreme type I PNe (He/H and N/O attaining very large values), but it shows very low oxygen, neon, sulphur, and argon abundances, all being consistent with an intermediate-mass progenitor formed in a low metallicity environment. The distance to IPHASX J012507.9+635652 is probably very large: a kinematic distance of $7.0^{+4.5}_{-3.0}$ kpc is derived from the Hα and [N II] radial velocities, yielding a huge galactocentric distance of $13.4^{+4.1}_{-2.5}$ kpc. This makes IPHAS J012507.9+635652 a rare and most valuable probe for chemical studies in the outer Galaxy.

Acknowledgements. This work is based on observations made with the INT and WHT telescopes operated on the island of La Palma by the Isaac Newton Group (ING) in the Spanish Observatorio del Roque de los Muchachos. INT and WHT observations were made during service time, and the excellent support from the ING staff is sincerely ackowledged. We thank J. A. López, M. Richer, and H. Riesgo for kindly acquiring the MESCAL spectra for us, and M. Santander García for the use of his spatio-kinematical programmes. A.M., R.L.M.C., K.V., E.R.R.F, and P.L. thank funding from the Spanish AYA2002-0883 grant. Finally, A.M. acknowledges the hospitality of the Instituto Nacional de Astrofísica, Óptica y Electrónica (INAOE, Puebla, México) and the Spanish M.E.C (grant PR 2004-0598) during his sabbatical leave in México.

References

Ann, H. B., & Lee, S. H. 2002, J. Korean Astron. Soc., 35, 29
Balick, B., & Frank, A. 2002, ARA&A, 40, 439
Blackman, E. G., Frank, A., & Welch, C. 2001, ApJ, 546, 288
Buzzoni, A., Arnaboldi, M., & Corradi, R. L. M. 2006, MNRAS, 368, 877
Cardelli, J. A., Clayton, G. C., & Mathis, J. S. 1989, ApJ, 345, 245
Casassus, S., Roche, P. F., & Barlow, M. J. 2000, MNRAS, 314, 657
Condon, J. J., Cotton, W. D., Greisen, E. W., et al. 1998, AJ, 115, 1693
Corradi, R. L. M. 2004, in Asymmetrical Planetary Nebulae III: Winds, Structure and the Thunderbird, ed. M. Meixner, J. H. Kastner, B. Balick, & N. Soker, ASP Conf. Ser., 313, 148
Corradi, R. L. M., & Schwarz, H. E. 1993, A&A, 268, 714
Corradi, R. L. M., Mampaso, A., Viironen, K., et al. 2005, in Planetary Nebulae as Astronomical Tools, ed. R. Szczerba, G. Stasińska, & S. K. Górny, AIP Conf. Proc., 804, 7
Costa, R. D. D., Uchida, M. M. M., & Maciel, W. J. 2004, A&A, 423, 199
Cuesta, L., & Phillips, J. P. 2000, ApJ, 543, 754
Cutri, R. M., Skrutskie, M. F., van Dyk, S., et al. 2003, 2MASS All Sky Catalog of point sources, 2003 VizieR Online Data Catalog
Drew, J. E., Greimel, R., Irwin, M. J., et al. 2005, MNRAS, 362, 753
Frew, D. J., Parker, Q. A., & Russeil, D. 2006, MNRAS, submitted
Guerrero, M. A., & Manchado, A. 1998, ApJ, 508, 262
Henry, R. B. C., & Howard, J. W. 1995, ApJ, 438, 170
Icke, V. 2003, A&A, 405, L11
Kaler, J. B., & Lutz, J. H. 1985, PASP, 97, 700
Kimeswenger, S., & Weinberger, R. 1989, A&A, 209, 51
Kingsburgh, R. L., & Barlow, M. J. 1994, MNRAS, 271, 257 (KB94)
Koeppen, J., Acker, A., & Stenholm, B. 1991, A&A, 248, 197
Lindoff, U. 1969, Arkiv för Astronomii, 5, 221
Livio, M., & Pringle, J. E. 1997, ApJ, 486, 835
Mampaso, A., Viironen, K., Corradi, R. L. M., et al. 2005, in Planetary Nebulae as Astronomical Tools, ed. R. Szczerba, G. Stasińska, & S. K. Górny, AIP Conf. Proc., 804, 14
Manchado, A. 2004, in Asymmetrical Planetary Nebulae III: Winds, Structure and the Thunderbird, ed. M. Meixner, J.H. Kastner, B. Balick, & N. Soker, ASP Conf. Ser., 313, 3
Manchado, A., Stanghellini, L., & Guerrero, M. A. 1996, ApJ, 466, L95
Marigo, P., Bernard-Salas, J., Pottasch, S. R., Tielens, A. G. G. M., & Wesselius, P. R. 2003, A&A, 409, 619 (Ma03)
Matsuura, M., Zijlstra, A. A., Molster, F. J., et al. 2005, MNRAS, 359, 383
Moe, M., & De Marco, O. 2006, ApJ, in press [arXiv:astro-ph/0606354]
Muthu, C., & Anandarao, B. G. 2001, AJ, 121, 2106
Negueruela, I., & Okazaki, A. T. 2001, A&A, 369, 108
Nordström, B., Mayor, M., Andersen, J., et al. 2004, A&A, 418, 989
Oke, J. B. 1990, AJ, 99, 1621
Parker, Q. A., Phillipps, S., Pierce, M. J., et al. 2005, MNRAS, 362, 689
Parker, Q. A., et al. 2006, MNRAS, submitted
Perinotto, M. 1991, ApJS, 76, 687
Perinotto, M., & Corradi, R. L. M. 1998, A&A, 332, 721
Perinotto, M., Morbidelli, L., & Scatarzi, A. 2004, MNRAS, 349, 793
Phillips, J. P. 2005, MNRAS, 361, 283
Pickles, A. J. 1998, PASP, 110, 863
Pierce, M. J., Frew, D. J., Parker, Q. A., & Köppen, J. 2004, Publications of the Astronomical Society of Australia, 21, 334
Pottasch, S. R. 1983, Planetary Nebulae, Astrophysics & Space Science Library, 107
Ramos-Larios, G. R., & Phillips, J. P. 2005, MNRAS, 357, 732
Rodríguez, M., Corradi, R. L. M., & Mampaso, A. 2001, A&A, 377, 1042
Rolleston, W. R. J., Smartt, S. J., Dufton, P. L., & Ryans, R. S. I. 2000, A&A, 363, 537
Sabbadin, F., Minello, S., & Bianchini, A. 1977, A&A, 60, 147
Sahai, R. 2004, in Asymmetrical Planetary Nebulae III: Winds, Structure and the Thunderbird, ed. M. Meixner, J.H. Kastner, B. Balick, & N. Soker, ASP Conf. Ser., 313, 141
Sahai, R., & Trauger, J. T. 1998, AJ, 116, 1357
Santander-García, M., Corradi, R. L. M., Balick, B., & Mampaso, A. 2004, A&A, 426, 185
Schlegel, D. J., Finkbeiner, D. P., & Davis, M. 1998, ApJ, 500, 525
Schmeja, S., & Kimeswenger, S. 2001, A&A, 377, L18
Schmidt-Kaler T. 1982, in Landolt-Bornstein: Numerical Data and Functional Relationships in Science and Technology, ed. K. Schaifers, & H. H. Voigt
Solf, J., & Ulrich, H. 1985, A&A, 148, 274
Sowell, J. R. 1987, ApJS, 64, 241
Torres-Peimbert, S., Peimbert, M., & Peña, M. 1990, A&A, 233, 540
Tsamis, Y. G., Barlow, M. J., Liu, X.-W., Danziger, I. J., & Storey, P. J. 2003, MNRAS, 345, 186
Vallée, J. P. 2002, ApJ, 566, 261
Warner, B. 1995, in Cataclysmic Variables, Cambridge Astrophysics Series No. 28 (Cambridge: CUP), 146
Whitelock, P. A. 1985, MNRAS, 213, 59

[1] Instituto de Astrofísica de Canarias, 38200 La Laguna, Tenerife, Spain
e-mail: amr@iac.es; kerttu@iac.es
[2] Isaac Newton Group. Ap. de Correos 321, 38700 Sta. Cruz de la Palma, Spain
e-mail: [rcorradi;pleisy;greimel]@ing.iac.es
[3] Imperial College, Blackett Laboratory, Exhibition Road, London, SW7 2AZ, UK
e-mail: j.drew@imperial.ac.uk
[4] University College London. Department of Physics and Astronomy. Gower St. London WC1E 6BT, UK
e-mail: mjb@star.ucl.ac.uk
[5] Department of Physics, Macquarie University, NSW 2109, Australia
e-mail: [dfrew;qap]@ics.mq.edu.au
[6] Cambridge Astronomical Survey Unit, Institute of Astronomy, Cambridge, UK
e-mail: jmi@ast.cam.ac.uk
[7] Astrophysics Group, Department of Physics, Bristol University, Tyndall Avenue, Bristol, BS8 1TL, UK
e-mail: [r.morris;s.phillipps]@bristol.ac.uk
[8] Instituto de Geofísica y Astronomía. Calle 212, No. 2906, CP 11600, La Habana, Cuba
e-mail: erflores@iga.cu
[9] School of Physics and Astronomy, Manchester Univ., Sackville Street, PO Box 88, Manchester M60 1QD, UK
e-mail: aaz@iapetus.phy.umist.ac.uk